75th International Astronautical Congress (IAC), Milan, Italy, 14-18 October 2024.

IAC–24–C1.3.2

UNCOOPERATIVE SPACECRAFT RELATIVE NAVIGATION VIA VISIBLE AND THERMAL-INFRARED IMAGE FUSION

Gaia Letizia Civardi [a*], **Massimiliano Bussolino** [a], **Matteo Quirino** [a], **Michele Bechini** [a], **Michèle Lavagna** [a]

[a] *Politecnico di Milano, Department of Aerospace Science and Technology, Via La Masa, 34, 20156, Milano - Italy*

[*] Corresponding Author: gaialetizia.civardi@polimi.it

The paper presents an effective and robust approach to enhance the flexibility of vision-based navigation strategies when operating in proximity of non-cooperative orbiting objects for In Orbit Servicing or Active Debris Removal missions. To improve vision-based navigation systems, our research introduces pixel level fusion of visible (VIS) and thermal-infrared (TIR) images. Our work aims at exploiting the reliability of TIR images even during eclipses, since they are less affected by illumination. The fused images are fed to a model-based navigation chain which is able to estimate the relative pose (position and attitude) between the chaser and the target. This navigation strategy is tested under challenging illumination conditions to highlight the benefits of multispectral data fusion with respect to a traditional VIS-only navigation strategy. Our research aims to advance towards a more robust navigation architecture capable of operating in challenging close-proximity operations.

Keywords: Thermal Infred Imaging, Image Fusion, Relative Navigation, Extended Kalman Filter

1. Introduction

In recent years, missions involving proximity operations between artificial objects in orbit have gained increasing attention, particularly for performing routine in-orbit services [1]. A key area of focus is the relative state estimation of a chaser spacecraft with respect to an uncooperative target, i.e. a target that lack light-emitting markers and cannot communicate with the chaser. While the relative pose (position and attitude) between spacecraft could theoretically be determined using ground-based tracking methods, this approach is hindered by significant uncertainties and is heavily dependent on the spacecraft's visibility from ground stations [2]. Consequently, ground-based methods are unsuitable for scenarios such as formation flying missions with fractionated scientific payloads, on-orbit servicing demonstrators, and active debris removal. Although further technological advancements are necessary to make these missions feasible, the high level of responsiveness required from the chaser during close proximity operations and maneuvering necessitates onboard estimation of the relative pose, relying solely on the chaser's capabilities. This means it is especially challenging to deal with uncooperative artificial targets, since it demands robustness in both standard and off-nominal operations. It is important to note that onboard pose estimation is merely the first step towards developing a fully autonomous guidance, navigation, and control (GNC) system, which ensures timeliness, reactivity, effectiveness, and robustness. Concerning the navigation sensor suite, monocular cameras represent the most attractive solution to collect meaningful GNC measurements while at the same time limiting both the sensor mass and its power consumption [3]. State-of-the art navigation strategies rely on cameras operating within the visible (VIS) spectrum. Extensive research has been conducted and several flight testes have been carried out to evaluate their performances in rendezvous scenarios involving both cooperative [4] and uncooperative [5]targets. Nevertheless, it must be acknowledged that VIS images are strongly affected by the illumination conditions. In case of eclipse or high Sun Phase Angle (SAA) the target spacecraft may be partially visible or almost not visible, while in case of direct illumination, depending on the relative Sun-Target-Camera geometry, saturation, flares and stray light noises may be present [6]. Both the aforementioned situations can jeopardize the whole navigation pipeline, especially for those missions orbiting in LEO, which are characterized by dynamical illumination conditions [7]. Recent studies [8] propose the introduction of a Thermal-Infrared (TIR) camera within the sensor suite to complement the VIS one. While VIS cameras sense light that is primarily reflected from a scene, TIR cameras sense light emitted by objects due to their natural temperature. Therefore, unlike VIS cameras, TIR cameras are more robust to ambient illumination conditions. However, TIR cameras generally have a smaller array size and a lower image contrast with respect to VIS ones, thus provid-

ing a lower quality image. Therefore, utilizing multispectral information in a complementary way, can enhance the navigation robustness when one sensing modality becomes degraded. The main contribution of this work is the development of a pose estimation chain which exploits VIS-TIR fused images. This study builds on previous works by the authors: in [9] the best image fusion algorithms for a ligthweight architecture are identified, while in [10] pose initialization is successfully performed on VIS-TIR fused images. Our work makes a step forward in the direction of a more robust navigation chain by successfully performing relative pose estimation through the exploitation of fused images and by proving its efficacy with respect to a traditional VIS-only optical navigation chain. The remainder of this paper is organized as follows: the available literature on the topics related to this article is reviewed in Sec. 2, while in Sec. 3 the navigation architecture is presented and described in details. The tools for VIS and TIR images generation used in the work are reported in Sec. 4, as well as the test plan. The results of the relative navigation architecture on VIS-TIR fused images are then shown in Sec. 5. The main conclusions and some hints for possible future developments are listed in Sec. 6.

2. Literature Review

2.1 Vision-based relative navigation

The relative pose estimation problem can be tackled by exploiting either a loosely-coupled or a tightly-coupled relative navigation architecture. In loosely coupled approaches, the navigation architecture is composed by two separate functional blocks. First, the pose determination block processes the acquired images to provide an estimate of the relative pose, which is then fed to the navigation filter. Within this context, the relative rotational and translational filters are separate, as in [11], to further enhance the robustness of the system. Tightly-coupled approaches instead directly process the information extracted from the acquired images within a filtering scheme, as shown in [12]. In our research we focus on a tightly coupled approach which matches the feature point positions on the image plane with a known 3D wireframe model. This approach enables us to have a lightweight image processing architecture, which only involves feature detection and feature tracking, and to directly exploit the EKF for both pose estimation and VIS-TIR data fusion.

2.2 VIS-TIR data fusion

The main objective VIS-TIR data fusion is to merge the complementary advantages of the two distinguished spectral bands and to enhance the navigation chain robustness to highly dynamical illumination conditions. Different strategies can be adopted to perform VIS-TIR data fusion, as outlined in [13]. Pixel-level image fusion aims at fusing the complementary information directly at image level to create a new and more informative image that can replace the ones belonging to the two separate spectra. Another option is represented by the so called *decision-level* data fusion, in which the two source images are processed separately, and then the extracted information is fused in a further stage, such as in a navigation filter. This approach has been already investigated in different works, such as [14] and [15]; showing good results in terms of accuracy and robustness. The proposed research instead focuses on an image fusion based navigation architecture, building on the previous work carried out by the authors [9], [10], [16], with the aim of filling this research gap and paving the way to a thorough comparison between the two data fusion strategies. Image fusion techniques aim at exploiting the strengths of sensors operating in different spectral bands to generate a robust and informative image that can ease the subsequent processing phase. Image fusion algorithms have already been applied to a wide range of application fields, such as object recognition, detection for surveillance [17] and remote sensing [18], yet they have never been applied within the context of spaceborne navigation. Different pixel-level image fusion algorithms exist and they can be grouped according to their baseline theory, as highlighted in [13]. In a previous work by the authors [9], different image fusion techniques are quantitatively compared on synthetically generated VIS and TIR images of the Tango spacecraft, with the aim of selecting the most effective algorithms to be incorporated into a visual navigation chain. From the findings of this research, it can be concluded that Multiscale-based methods emerge as the best option due to their high effectiveness and low computational demand. These algorithms are characterized by three common steps: the two source images are first decomposed into components at different scales using techniques such as pyramidal transformation or edge preserving filters. Then, the multi-scale representations of the VIS and TIR images are fused according to a given fusion rule, such as a weighted average. Lastly, the fused image is obtained through the inverse multi-scale transform.

3. Navigation Architecture

A schematic representation of the proposed visual-based navigation architecture is reported in 1. The image fusion functional block performs pixel-level image fusion; the image processing block performs feature detection and track-

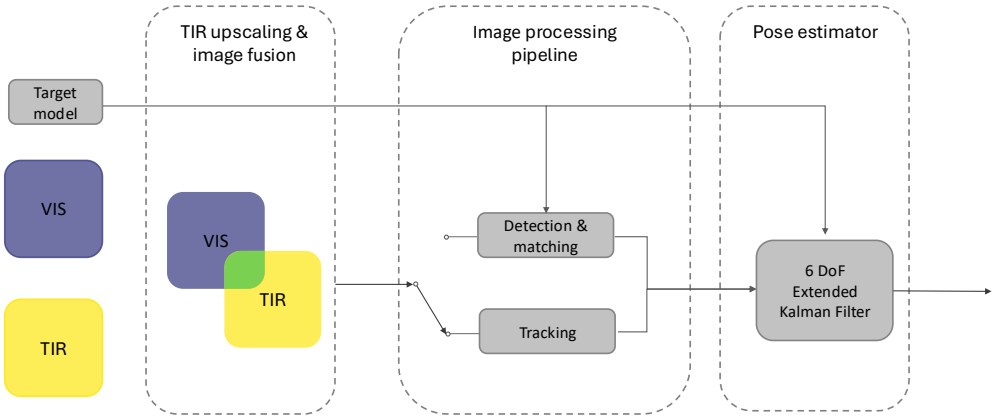

Fig. 1: Navigation chain architecture

ing; while an Extended Kalman Filter (EKF) processes the measurements to estimate the relative chaser-target pose. The filter relies on the target point-feature positions on the image plane as measurements and it estimates the relative pose by comparing them to the expected position of the matched target model's landmarks projection on the image plane. Our EKF exploits a coarse target model which is available offline, which may be representative of an approach phase which exploits the results gathered during the inspection phase. Similar strategies were adopted in previous works, as outlined in [19], [20].

3.1 Image Fusion

Image fusion techniques require the two source images to have the same resolution. As discussed in [9], upscaling TIR images before the fusion step achieves higher quantitative performance metrics rather than downscaling VIS images. Bicubic interpolation [21] is employed in this work. As mentioned in Sec. 2, multiscale-based fusion methods have been identified as the best solution to perform pixel level image fusion. Specifically, we employ an algorithm inspired by that presented in [22]. First the source images are decomposed into a base layer and a detail layer through convolution with an averaging image filter. The fusion weights used to merge the detail layers are based on the saliency maps of the source images. The main difference between our implementation and the reference one is that in the original work, median and mean image filters are employed, our version uses image convolution with a Scharr filter. The Scharr gradient reflects the significant structural features of an image, such as edges, outlines, and region boundaries and it is resilient with respect to image noise. A simple average rule is here used to perform base layer fusion. In this way, the resulting fused image is rich in details and it effectively retains the bright regions of the TIR image.

3.2 Image Processing

The image processing functional block is in charge of extracting features and tracking them across the incoming images. Periodically, feature re-initialization is performed. Among different feature detectors, ORB [23] has been selected for this work to be applied both to VIS and TIR images; due to its robustness to challenging illumination conditions and scale variations. The number of features is restrained to 250 to reduce the computational burden. The detected feature points are then tracked across the subsequent images using Lucas-Kanade tracking algorithm [24]. The number of tracked features decreases throughout the sequence images due to the relative motion between the chaser and the target. To keep the number of tracked features high enough to ensure a reliable pose estimation, a dedicated routine is implemented to detect and match new features to be added to the already tracked set. A detailed explanation of the feature re-initialization routine is available in [25], while it is here omitted for brevity.

3.3 Navigation Filter

The filter is designed to estimate the relative position, velocity, attitude and angular rates of the target with respect to the chaser spacecraft. Since the observation model depends on both the relative position and attitude, the navigation filter needs to be coupled. The state vector is defined as:

$$\boldsymbol{x} = \begin{bmatrix} \boldsymbol{\varrho}^T, & \dot{\boldsymbol{\varrho}}^T, & \boldsymbol{q}^T, & \boldsymbol{\omega}^T \end{bmatrix}^T \tag{1}$$

being $\boldsymbol{\varrho}$ and $\dot{\boldsymbol{\varrho}}$ the relative position and velocity between the two spacecraft's centers of mass, $\boldsymbol{q}$ the relative quaternion and $\boldsymbol{\omega}$ the relative angular velocity. The relative translational dynamics relies on a simple Clohessy-Whiltshire model [26], which is expressed in the chaser Local Vertical Local Horizon (LVLH) reference frame. The attitude parametrization follows the formulation of a Multiplicative Extended Kalman Filter (MEKF) [27]. The filter propagates a three-element local attitude error $\boldsymbol{a}$ formalized in Modified Rodrigues Parameters (MRP) while keeping track of a reference quaternion. The filter processes the projected positions of the target's model landmarks onto the image plane, according to Eqn. 2

$$\boldsymbol{p}_i = K(\boldsymbol{A}_{\mathcal{C}/\mathcal{T}}\boldsymbol{P_i} + \boldsymbol{\varrho}) \tag{2}$$

In which $\boldsymbol{P_i}$ is the i-th feature point position in the target's reference frame, $\boldsymbol{A}_{C/T}$ is the relative target-chaser attitude matrix and K is the intrinsic camera calibration matrix. A more detailed derivation of the observation model is available in [25] for the interested reader. The target's landmarks are the vertices of a reduced CAD model of its shape. In the case of the target Tango, this model contains 170 vertices.

4. Simulation Environment

This section is devoted to the description of our simulation environment and of the testing strategy employed to assess the performances of the proposed navigation algorithm.

4.1 Image Rendering

This work employs the open-source POV-Ray [28] to generate photorealistic spaceborne validated VIS images, as described in [29]. For the TIR images, Blender has been preferred as the main image rendering software, exploiting a tool internally developed by the ASTRA research group [30], [31]. The images produced using such tools are reported in Fig. 2 where the VIS images (Top) are compared with the TIR images (Middle) and the fused images (bottom) for a simplified Tango spacecraft model and the camera parameters reported in Table 1.

Concerning the noise level of the synthetically generated images, VIS images are postprocessed by adding a white Gaussian noise with σ^2= 0.0022 and blurred with a Gaussian blurring characterized by σ^2 = 1 and zero mean. The noise parameters have been selected equal to [32]. The TIR images are characterized by both a white Gaussian noise, whose variance has been set equal to the value used for the VIS images, and a pink noise [33], whose generation is detailed in [9].

	Array Size $[px]$	FoV $[deg]$	Focal Length $[mm]$
VIS	1024×1024	[14,14]	20
TIR	512×512	[14,14]	20

Table 1: VIS and TIR camera parameters.

4.2 Test Plan

The main objective of this work is to highlight the benefits of introducing TIR sensing within the navigation chain, therefore it is necessary to test the navigation algorithm against challenging illumination conditions. Our reference trajectory is representative of a relative closed orbit, with inter-satellite distance that ranges from a minimum of 10m up to a maximum of 15m, approximately. This trajectory is integrated by means of a two body dynamical model which accounts for the J_2 perturbation, solar radiation pressure and drag effect for both the chaser and the target spacecraft. The target initial angular velocity is set to $0.5deg/s$ around each axis and the attitude evolution is computed by means of the unperturbed euler equations. Target pointing is enforced for the chaser through a PID controller. A montecarlo simulation of 500 runs is then performed considering three different cases:

1. VIS-only, low SAA: the target spacecraft is always well illuminated.
2. VIS-only, high SAA: eclipses period occur.
3. VIS-TIR fusion: the navigation relies on fused VIS-TIR images. The VIS images are those related to the second test case.

5. Results

To quantify the navigation algorithm performances, the overall position error is computed as:

$$e_\rho = \sqrt{(x_i - \hat{x}_i)^2 + (y_i - \hat{y}_i)^2 + (z_i - \hat{z}_i)^2} \tag{3}$$

where $\hat{x}$,$\hat{y}$,$\hat{z}$ are the position components estimates. The percentage error on the true inter-satellite range is then ob-

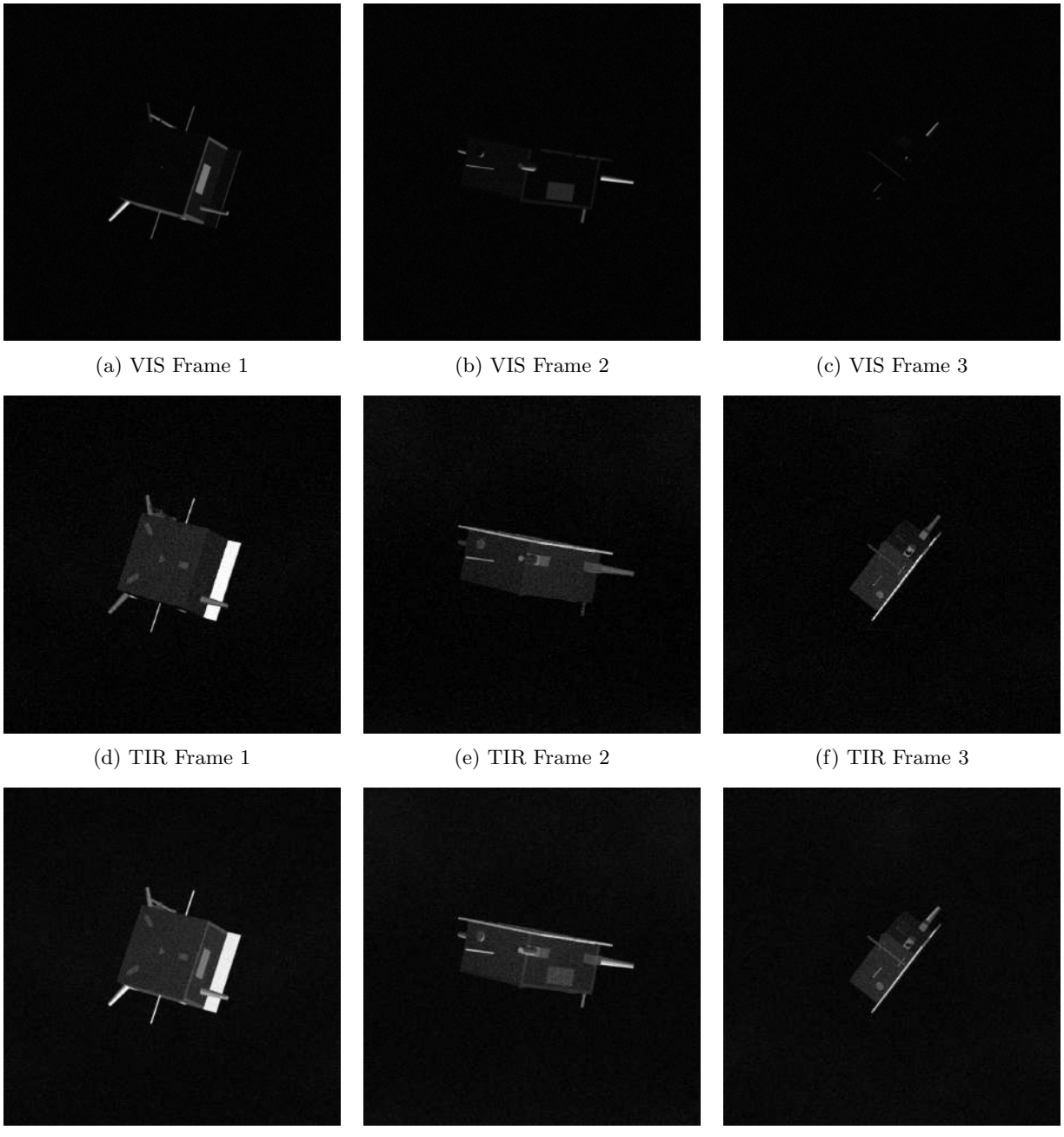

(a) VIS Frame 1 (b) VIS Frame 2 (c) VIS Frame 3

(d) TIR Frame 1 (e) TIR Frame 2 (f) TIR Frame 3

(g) FUS Frame 1 (h) FUS Frame 2 (i) FUS Frame 3

Fig. 2: VIS synthetic images (Top), TIR synthetic images (middle) and images (bottom).

tained, in order to achieve a normalized error metrics. The attitude error is instead computed following [34]:

$$e_R = arccos\left(1 - \frac{tr(\mathbf{I} - \mathbf{A}^T\hat{\mathbf{A}})}{2}\right) \quad (4)$$

The average position and attitude errors are reported in Fig.3 and Fig.4, respectively. The quantitative results are reported in Tab. 2. It can be noticed that the VIS-only navigation solution becomes highly unreliable when the SAA increases. In fact, both the position and attitude errors increase as the

Test case	Position [%]	Attitude [deg]
1	0.20 ± 0.16	1.70 ± 1.77
2	12.46 ± 4.11	9.62 ± 3.58
3	0.23 ± 0.21	1.81 ± 1.86

Table 2: Position and attitude errors.

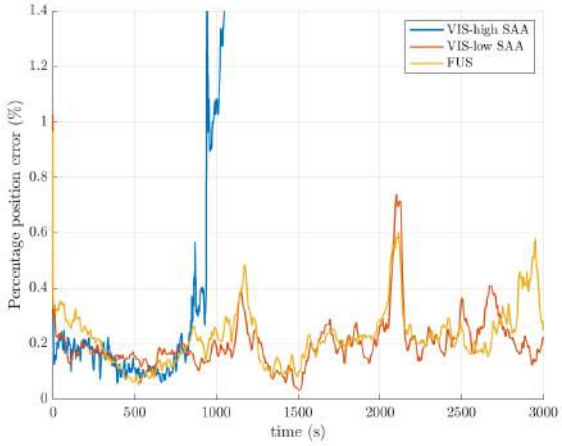

Fig. 3: Mean position error.

filter diverge. However, when the SAA is low, the VIS sensing modality provides accurate results both in terms of position and attitude. It should be pointed out that this test case represents an ideal condition, which is hardly ever encountered during close proximity operations. Concerning the data fusion strategy, it can be stated that the FUS navigation mode offers results which are comparable to the VIS case in ideal conditions. This finding underlines the validity of the proposed approach and the reliability of classical IP techniques even on fused VIS-TIR images. It is also worth mentioning the fact that the image fusion algorithm has not been tuned specifically to adapt to the presented image dataset, and that its settings have been kept constant throughout the whole simulation. This result further underlines the flexibility of the VIS-TIR image fusion scheme, which is able to provide informative images in any illumination conditions.

To offer a more in-depth insight in the performances of the data fusion navigation architecture, we also report the results of the montecarlo simulation for the test case n.3. Fig. 5 and Fig. 6 report the position and attitude estimation errors, respectively. The colored line represents the averaged result over the number of montecarlo runs. It can be noticed that the convergence transient is extremely short both for the position and attitude error estimation. There is an

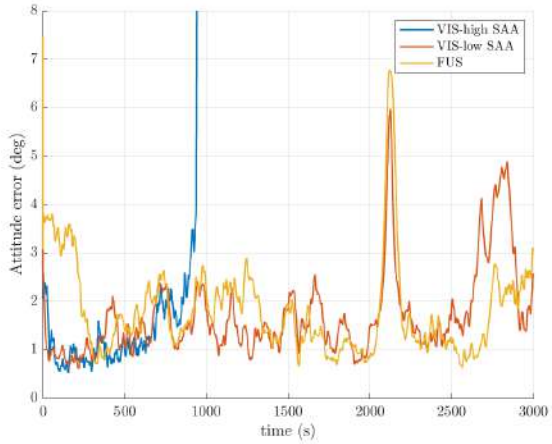

Fig. 4: Mean attitude error.

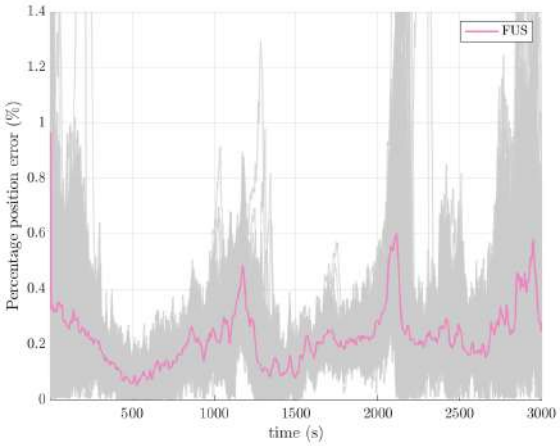

Fig. 5: Mean position error.

error increase towards the end of the simulation, which was present also in the test case n.1. This sudden error spike is not linked to the data fusion algorithms; it is instead due to the relative chaser-target orientation, which jeopardizes the feature tracking and feature detection algorithms. Nevertheless, after this challenging configuration, the filter is able to go back to its steady state error without diverging.

e

6. Conclusion

We present a navigation chain for estimating the relative pose between a chaser and an uncooperative target using fused visible and thermal infrared images. The proposed

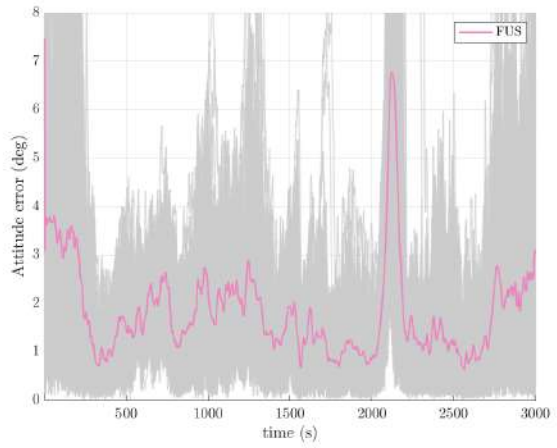

Fig. 6: Mean attitude error.

navigation solution allows for a satisfactory estimation of the relative state and angular velocity. The numerical evaluation of the presented approach confirms that a thermal camera is beneficial to the navigation chain when the illumination conditions are challenging; since it allows to reach results comparable to an ideal illumination condition. Further, we demonstrate that the image fusion approach is a valid data fusion strategy, since the fused VIS-TIR images were handled well by classical image processing algorithms. Image fusion techniques are indeed able to produce an informative images throughout the whole simulation, without requiring any specific tuning according to the dataset. These results underline the fact that multispectral sensing is a powerful resource during close proximity operations, where the illumination conditions change dynamically. The outcome of this research represents a step forward towards a flexible navigation strategy capable of dealing with any illumination conditions, enabling autonomous operations with uncooperative resident space objects. A step further in this research field requires the development and tailoring of image processing techniques to both thermal infrared images and to fused images to enhance the accuracy of the navigation solution.

References

[1] David K. Geller. Orbital rendezvous: When is autonomy required? *Journal of Guidance, Control, and Dynamics*, 30(4):974–981, 2007.

[2] Massimo Piazza, Michele Maestrini, and Pierluigi Di Lizia. Monocular relative pose estimation pipeline for uncooperative resident space objects. *Journal of Aerospace Information Systems*, 19(9):613–632, 2022.

[3] Roberto Opromolla, Giancarmine Fasano, Giancarlo Rufino, and Michele Grassi. A review of cooperative and uncooperative spacecraft pose determination techniques for close-proximity operations. *Progress in Aerospace Sciences*, 93:53–72, 2017.

[4] Manny R. Leinz, Chih-Tsai Chen, Michael W. Beaven, Thomas P. Weismuller, David L. Caballero, William B. Gaumer, Peter W. Sabasteanski, Peter A. Scott, and Mark A. Lundgren. Orbital Express Autonomous Rendezvous and Capture Sensor System (ARCSS) flight test results. In Richard T. Howard and Pejmun Motaghedi, editors, *Sensors and Systems for Space Applications II*, volume 6958 of *Society of Photo-Optical Instrumentation Engineers (SPIE) Conference Series*, page 69580A, April 2008.

[5] Francesco Castellini, David Antal-Wokes, Ramon Pardo de Santayana, Klaas, and Vantournhout. Far approach optical navigation and comet photometry for the rosetta mission. *Proceedings of 25th International Symposium on Space Flight Dynamics, 25th ISSFD*, 2015.

[6] Tae Ha Park, Marcus Märtens, Gurvan Lecuyer, Dario Izzo, and Simone D'Amico. Speed+: Next-generation dataset for spacecraft pose estimation across domain gap. In *2022 IEEE Aerospace Conference (AERO)*, pages 1–15. IEEE, 2022.

[7] Wigbert Fehse. Rendezvous with and capture / removal of non-cooperative bodies in orbit: The technical challenges. *Journal of Space Safety Engineering*, 1(1):17–27, 2014.

[8] Özgün Yilmaz, N Aouf, L Majewski, M Sanchez-Gestido, and G Ortega. Using infrared based relative navigation for active debris removal. In *10th International ESA Conference on Guidance, Navigation and Control Systems*, volume 29, 2017.

[9] Gaia Letizia Civardi, Michele Bechini, Matteo Quirino, Piccinin Margherita, Colombo Alessandro, and Michéle Lavagna. Generation of fused visible and thermal-infrared images for uncooperative spacecraft proximity navigation. *Advances in Space Research*, 2023.

[10] Michele Bechini, Gaia Letizia Civardi, Matteo Quirino, Alessandro Colombo, and Michéle Lavagna.

Robust monocular pose initialization via visual and thermal image fusion. In *73rd International Astronautical Congress (IAC 2022), International Astronautical Federation, IAF, Paris, France*, pages 1–15, 09 2022.

[11] Massimo Piazza, Michele Maestrini, and Pierluigi Di Lizia. Monocular relative pose estimation pipeline for uncooperative resident space objects. *Journal of Aerospace Information Systems*, 19(9):613–632, 2022.

[12] Lorenzo Pasqualetto Cassinis, Robert Fonod, Eberhard Gill, Ingo Ahrns, and Jesus Gil Fernandez. Comparative assessment of image processing algorithms for the pose estimation of uncooperative spacecraft. In *Proc. Int. Workshop Satell. Constellations Formation Flying*, pages 1–20, 2019.

[13] Jiayi Ma, Yong Ma, and Chang Li. Infrared and visible image fusion methods and applications: A survey. *Information Fusion*, 45:153–178, 2019.

[14] M Bussolino, M Piccinin, GL Civardi, M Lavagna, et al. Multispectral vision based relative navigation to enhance space debris proximity operations. In *International Astronautical Congress: IAC Proceedings*, pages 1–15, 2023.

[15] Federica Vitiello, Flavia Causa, Roberto Opromolla, and Giancarmine Fasano. Radar/visual fusion with fuse-before-track strategy for low altitude non-cooperative sense and avoid. *Aerospace Science and Technology*, 146:108946, 2024.

[16] Alessandro Colombo, Gaia Letizia Civardi, Michele Bechini, Matteo Quirino, and Michéle Lavagna. Vistir cameras data fusion to enhance relative navigation during in orbit servicing operations. In *73rd International Astronautical Congress (IAC 2022), International Astronautical Federation, IAF, Paris, France*, pages 1–15, 09 2022.

[17] Praveen Kumar, Ankush Mittal, and Padam Kumar. Fusion of thermal infrared and visible spectrum video for robust surveillance. In Prem K. Kalra and Shmuel Peleg, editors, *Computer Vision, Graphics and Image Processing*, pages 528–539, Berlin, Heidelberg, 2006. Springer Berlin Heidelberg.

[18] G. Simone, A. Farina, F.C. Morabito, S.B. Serpico, and L. Bruzzone. Image fusion techniques for remote sensing applications. *Information Fusion*, 3(1):3–15, 2002.

[19] Lorenzo Pasqualetto Cassinis, Robert Fonod, Eberhard Gill, Ingo Ahrns, and Jesús Gil-Fernández. Evaluation of tightly- and loosely-coupled approaches in cnn-based pose estimation systems for uncooperative spacecraft. *Acta Astronautica*, 182:189–202, 2021.

[20] Vincenzo Pesce, Roberto Opromolla, Salvatore Sarno, Michèle Lavagna, and Michele Grassi. Autonomous relative navigation around uncooperative spacecraft based on a single camera. *Aerospace Science and Technology*, 84:1070–1080, 2019.

[21] R. Keys. Cubic convolution interpolation for digital image processing. *IEEE Transactions on Acoustics, Speech, and Signal Processing*, 29(6):1153–1160, 1981.

[22] Durga Prasad Bavirisetti and Ravindra Dhuli. Two-scale image fusion of visible and infrared images using saliency detection. *Infrared Physics & Technology*, 76:52–64, 2016.

[23] Ethan Rublee, Vincent Rabaud, Kurt Konolige, and Gary Bradski. Orb: An efficient alternative to sift or surf. In *2011 International Conference on Computer Vision*, pages 2564–2571, 2011.

[24] Bruce Lucas and Takeo Kanade. An iterative image registration technique with an application to stereo vision. In *A Proceedings of the 7th International Joint Conference on Artificial Intelligence (IJCAI '81)*, volume 81, pages 1–24, 04 1981.

[25] Massimiliano Bussolino, Gaia Letizia Civardi, Matteo Quirino, Michele Bechini, and Michèle Roberta Lavagna. Cross-spectral navigation with sensor handover for enhanced proximity operations with uncooperative space objects. *Sensors*, Special Issue: Multi-sensor Fusion for Positioning and Navigation of Aerospace Vehicles:52–64, 2024.

[26] W. H. Clohessy and R. S. Wiltshire. Terminal guidance system for satellite rendezvous. *Journal of the Aerospace Sciences*, 27(9):653–658, 1960.

[27] John L. Crassidis and John L. Junkins. *Optimal Estimation of Dynamic Systems*. Chapman and Hall/CRC, April 2004.

[28] Tomas Plachetka. Pov ray: persistence of vision parallel raytracer. In *Proc. of Spring Conf. on Computer Graphics, Budmerice, Slovakia*, volume 123, page 129, 1998.

[29] Michele Bechini, Michèle Lavagna, and Paolo Lunghi. Dataset generation and validation for spacecraft pose estimation via monocular images processing. *Acta Astronautica*, 204:358–369, 2023.

[30] Matteo Quirino and Michèle Roberta Lavagna. Spacecraft and asteroid thermal image generation for proximity navigation and detection scenarios. *Applied Sciences*, 14(13), 2024.

[31] Matteo Quirino. *Novel thermal imges generator for autonomous space proximity operations*. Phd thesis, Politecnico di Milano, 2023.

[32] Mate Kisantal, Sumant Sharma, Tae Ha Park, Dario Izzo, Marcus Märtens, and Simone D'Amico. Satellite pose estimation challenge: Dataset, competition design, and results. *IEEE Transactions on Aerospace and Electronic Systems*, 56(5):4083–4098, 2020.

[33] E Brageot, O Groussin, P Lamy, and J-L Reynaud. Experimental study of an uncooled microbolometer array for thermal mapping and spectroscopy of asteroids. *Experimental Astronomy*, 38(3):381–400, 2014.

[34] Landis Markley and D. Mortari. Quaternion attitude estimation using vector observations. *Journal of the Astronautical Sciences*, 48, 04 2000.